COBEM 2023 27TH INTERNATIONAL CONGRESS OF MECHANICAL ENGENEERING

ABCM Brazilian Society of Mechanical Sciences and Engineering
27th ABCM International Congress of Mechanical Engineering
December 04-08, 2023, Florianópolis-SC, Brazil

COB-2023-0323
ENHANCEMENT HEAT TRANSFER IN A FLAT PLATE SOLAR COLLECTOR WITH A CORRUGATED TUBE UNDER THE THERMOSYPHON EFFECT

Ewerton Ferreira Lopes*
Leandro Oliveira Salviano**
São Paulo State University, Ilha Solteira, SP, Brazil.
ewertonferreiralopes@gmail.com*
leandro.salviano@unesp.br**

Abstract. *The development of new technologies for the generation and use of energy has been increasing significantly. In this scenario, the use of flat plate solar collectors to convert solar energy into thermal energy for heating water for residential and commercial purposes has been pleasing and promoted a reduction in residential electricity consumption of up to 40%. A promising but underexplored area in engineering is the study of the intensification of heat transfer in these devices by changing the dimensional and constructive characteristics of the elevation tubes, especially through a numerical approach to passive systems that operate under the thermosyphon effect. Thus, this work aims to investigate, by using Computational Fluid Dynamics (CFD), the heat transfer process in a flat plate solar collector with a concentric plate to the elevation tube, evaluating different diameters, angles of inclination, and slope corrugation profiles subjected to a constant heat flux. The numerical modeling considers a single-phase, incompressible, permanent, three-dimensional and laminar flow, in addition to the Boussinesq approximation. The results showed that significant increases in the heat transfer rate can be achieved with absorber plates in comparison to those configurations without absorber plates. Moreover, the increase of the tube diameter allowed gains of up to 5.1% in the heat transfer rate, while the increase of the angle of inclination did not promote significant improvements. The triangular profile R10 P20 configuration increased the Nusselt number by 8%, while the R5 P20 configuration promoted a 25% gain in thermohydraulic performance.*

Keywords: *Solar Energy, Flat Plate Solar Collector, Corrugated Tube, Thermosyphon Effect, CFD.*

1. INTRODUCTION

The growing global demand for energy has fostered the development of new technologies for generating and utilizing the resource. In this scenario, the use of solar thermal energy through flat plate solar collectors for water heating has gained projection, mainly for using in domestic and commercial applications, where the required operating temperature is less than 100 ºC. According to the 2022 Solar Heat Worldwide Report, the global capacity to convert solar thermal energy into thermal energy through collectors increased from 62 GW_{th} in 2000 to 522 GW_{th} in 2021.

Brazil appears as a potential player in the use of solar thermal energy due to its advantageous geographic location (Pereira et al., 2017). The country's total installed capacity for converting solar thermal energy into thermal energy increased by 28% in 2021. Water heating for residential purposes, mainly through the use of electric showers, is considered the main responsible for the increase in electricity consumption. To replace or reduce the use of these devices, flat plate solar collectors are an alternative (Shukla et al., 2013). This type of demand represents 30% to 40% of residential electricity consumption (ABRASOL, 2022).

In solar water heating systems, fluid circulation can occur naturally (passive system) or by force (active system). Passive systems operate under the thermosyphon effect, where the flow is maintained through a density gradient that comes from the temperature difference caused by solar radiation (Agunlejika et al., 2016). This kind of system has been widely employed in the home and commercial sectors due to its simplicity—consisting of a thermal reservoir, connecting tubes, and a flat plate solar collector—and the low cost of acquisition and maintenance. Active systems are instrumented, use electric pumps, valves and temperature controllers to promote flow (Jamar et al., 2016), which makes them less alluring financially.

The flat plate solar collector is the stationary thermal component in solar water heating systems responsible to transfer solar thermal energy to the water. Most studies that seek to increase heat transfer in flat plate solar collectors involve changing the standard design of the devices like Visa et al. (2019); adding enhancement devices to the system that can act on the surface, such as selective solar coatings like Müller et al. (2019), or directly on the flow, either through addition of nanofluids like Zayed et al. (2019) or insertion of turbulator devices and vortex generators in elevation tube like Vijay et al. (2021).

The use of corrugated tubes as a passive technique to intensify heat transfer has been adopted in several areas of the chemical, food and automotive industries, among others. In a simple and inexpensive way, corrugations provide enhancement to heat transfer with moderate pressure drop (Andrade et al., 2019). Normally, corrugations are classified according to their arrangement, helical or transverse type, and dimensionally characterized by the height (e) and pitch (p) of the corrugation. As a method of intensification, undulations can promote secondary flows or cause separation and re-fixation of the fluid-dynamic boundary layer, depending on the crest shape and Reynolds number (Vicente et al., 2004)

For systems subjected to forced convection and low Reynolds numbers, the corrugated configurations examined by Rainieri et al. (1996) and Barba et al. (2002), demonstrated a ratio greater than unity between the enhancement heat transfer (Nusselt number) and the pressure drop penalty (friction factor). The results of Andrade et al. (2019) demonstrate that, in the laminar regime, the higher the Reynolds number, the larger the benefits in heat transfer that the corrugated tubes promote. The same pattern was seen in the turbulent regime by Mohammed et al. (2013) and Chen et al. (2013). According to Rainieri and Pagliarini (2002), if Re $\leq$ 200, both types of corrugations (transverse and helical) do not promote gains to the Nusselt number. However, for higher values, Re $\geq$ 400, transverse corrugations with smaller pitches, presented a higher periodicity of interruption of the development of the fluid-dynamic boundary layer, anticipating the transition of the flow regime. In addition, the results obtained for high wall heat flux showed a greater ability of transverse corrugations to increase heat transfer by convection in low Reynolds number ranges. The research by Cruz et al. (2021) shows that for helical corrugations, the Nusselt number obtained by corrugated tubes in the laminar regime is comparable to the outcomes produced by smooth tubes. According to the investigations by Andrade et al. (2019) and García et al. (2012), the change of the flow regime for helical corrugations is only demonstrated for Re $\geq$ 1000. The computational analysis performed by Du et al. (2018) and the experimental research by Vicente et al. (2004) emphasize that the height of the helical corrugations has a significant impact on the transition of the flow regime.

Although the use of corrugated tubes has been shown to be a viable alternative for thermal improvement in a number of applications, nothing is known about how this method affects the heat transfer process in flat plate solar collectors that operate under the thermosyphon effect. Therefore, the main objective of this study is to investigate through Computational Fluid Dynamics (CFD) the heat transfer process in a flat plate solar collector with corrugated elevatation tubes. For this, initial setups using non-corrugated elevated tubes with diameters of 9.52 mm, 12.07 mm, and 19.05 mm, inclined at 20°, 30°, 45°, and 60°. The configuration that offers the best thermo-hydraulic performance to the system will be used as a reference for evaluating the impact promoted by tubes with cross corrugations on the heat transfer rate and the thermo-hydraulic performance of the collector. Three corrugation profiles (circular, triangular and elliptical) with four pitch and corrugation height settings will be evaluated. The cases will be modeled with continuous heat flux, allowing the flow to develop only as a result of the thermosyphon effect.

2. COMPUTATIONAL MODELING

2.1 Governing equations and thermo-hydraulic parameters

The modeling of heat transfer and flow dynamics in a solar collector under the thermosyphon effect was carried out using the Finite Volume methodology in the commercial software ANSYS Fluent. The hypotheses of single-phase, incompressible, three-dimensional and steady-state flow were considered, in addition to the Boussinesq approximation, suitable for the characterization of natural convection in the interior of ducts, also employed in the studies of Ghsemi et al. (2012). The viscous dissipation term was ignored because of the low velocities connected to natural convection currents. As a result, the equations for continuity, momentum, and energy are, respectively:

$$\frac{\partial}{\partial x_i}(u_i) = 0 \tag{1}$$

$$\frac{\partial}{\partial x_j}(u_i u_j) = g_i(\Delta\rho/\rho) + \frac{\partial}{\partial x_j}\left(\nu \frac{\partial u_i}{\partial x_j}\right) \tag{2}$$

$$\frac{\partial}{\partial x_i}\left(u_i c_p T - k\frac{\partial T}{\partial x_i}\right) = 0 \tag{3}$$

The energy conservation equation in the solid sections of the domain (absorber plates) is defined by Eq. (4).

$$\nabla.(k\,\nabla T) = 0 \tag{4}$$

The Boussinesq model, Eq. (5), treats density as a constant in all solved equations, except for the buoyancy term in the equation of momentum. The model is defined as:

$$(\rho - \rho_o)g \approx -\rho_o \beta (T_s - T_e)g \tag{5}$$

The Second-Order Upwind Scheme is used to discretize the viscous terms of the momentum equations, the scheme calculates the quantities on cell faces using a multidimensional linear reconstruction approach by Barth and Jespersen (1989). The Couple algorithm, which simultaneously solves the momentum and continuity equations based on pressure, was utilized to solve the pressure-velocity coupling. For pressure interpolation, the PRESTO! Scheme was used (PREssure Staggering Option). The method uses discrete continuity balance for an inertial control volume over the face to compute the face pressure. Computational convergence is ensured for residuals smaller than 10^{-4} for the continuity equation, 10^{-5} for the momentum and 10^{-7} for the energy equation.

The flow is characterized by Reynolds number, based on the tube diameter, Eq. (6). The characterization of the thermo-hydraulic performance is accomplished by Nusselt number and friction factor, defined by Eq. (7) and (8).

$$Re = \frac{\rho u D}{\mu} \tag{6}$$

$$Nu = \frac{hD}{k} \tag{7}$$

$$\mathrm{f} = \frac{2\Delta P}{\rho u^2}\frac{D}{L_t} \tag{8}$$

The heat transfer rate, pressure drop and convective heat transfer rate are determined by Eq. (9), Eq. (10) and Eq. (11), respectively.

$$\dot{q} = q''.A_t \tag{9}$$

$$\Delta P = \bar{P}_{in} - \bar{P}_{out} \tag{10}$$

$$h = \frac{q''}{\bar{T}_w - \bar{T}_m} \tag{11}$$

where,

$$\bar{P} = \frac{\iint p dA}{\iint dA} \tag{12}$$

$$\bar{T} = \frac{\iint uTdA}{\iint udA} \tag{13}$$

2.2 Computational domain and boundary conditions

The flat plate solar collector considered in the work has absorber plates concentric to the elevated tubes, similar to the model evaluated by Jaisankar et al. (2011). Comparative studies between collectors of this type with different arrangements of absorber plates are scarce in the literature. However, most of the low-cost models sold in Brazil have this configuration. To reduce computational processing costs and numerical convergence time, the modeling considers one section of the collector, with a single tube and two plates, as shown in Figure 1. The thermo-hydraulic impact of tube diameter and inclination angle on the system is evaluated for 9.52 mm, 12.70 mm, and 19.05 mm diameter tube configurations, with concentric absorber plates 1 mm thick, 100 mm wide, and 1000 mm long. All tubes are evaluated at an angle of 20°, 30°, 45° and 60° in relation to the horizontal.

The pressure inlet and outlet are imposed at the inlet and outlet of the numerical domain of the tube. Constant heat flux equivalent to 750 W/m² is applied on the surface of the tube and absorber plates, while the bottom and sides of the collector are thermally insulated to avoid thermal losses. The bottom surface of the tube and the absorber plates, as well as the lateral faces of the plates are considered adiabatic in the numerical modeling, except for the interface between the tube and the absorber plates, which allows heat conduction between the components. To stabilize the numerical solution, extensions were added upstream and downstream of the tubes with lengths of 100 mm and 1000 mm, respectively. The slip condition is imposed on the surface of the extensions.

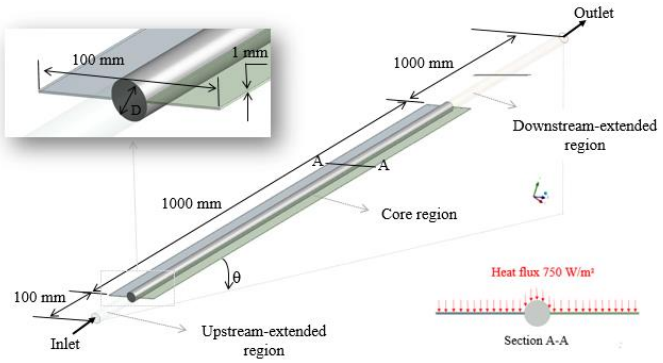

Figure 1. Computational domain.

Figure 2 shows the three corrugated profiles evaluated (circular, triangular and elliptical). The dimensionless height (*e/D*) of the profiles implies a reduction of 5% (R5) and 10% (R10) of the nominal diameter of the riser pipe. For each corrugation height, configurations with pitch of 10 mm (P10) and 20 mm (P20) are evaluated.

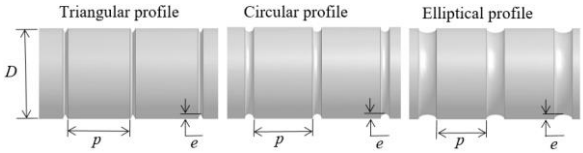

Figure 2. Corrugated profiles.

2.3 Grid independence and numerical validation

The Grid Convergence Index (GCI), introduced by Celik et al. (2008), is used to assess the numerical uncertainty of the computational domain's discretization. As a function of three stages of mesh refinement, the method measures the discretization errors of different parameters of interest in the numerical model. The Nusselt number, pressure drop, and mass flow are the relevant parameters in this work. The refinement factor (r) that quantifies the level of refinement between the meshes must be greater than or equal to 1.30 is ensured, according to Table 1

Table 1. Characteristics of each grid.

Tube diameter [mm]		**Number of cells**	**Refinement factor** $\boldsymbol{r = (\frac{G_{n+1}}{G_n})^{\frac{1}{3}}}$
Ø9.52	Grid 3 (G_3)	1623900	-
	Grid 2 (G_2)	3605800	1.30
	Grid 1 (G_1)	8359000	1.32
Ø12.70	Grid 3 (G_3)	1613700	-
	Grid 2 (G_2)	3570000	1.30
	Grid 1 (G_1)	8025900	1.31
Ø19.05	Grid 3 (G_3)	1656700	-
	Grid 2 (G_2)	3624400	1.30
	Grid 1 (G_1)	8186300	1.31

The results of the parameters of interest submitted to the GCI method, refer to the simulations of prototypes with corrugated tubes (with a diameter of 9.52 mm, 12.70 mm and 19.05 mm) and concentric absorber plates, inclined at 45° in relation to the horizontal. The numerical uncertainty obtained by ($GCI_{r_{32}}$) shown in Table 2, presents thermo-hydraulic results lower than 2% and comparable to those obtained by the more refined mesh ($GCI_{r_{21}}$) with a significantly smaller element number. As a result, the intermediate mesh is defined as the default.

Table 2. Grid convergence index.

Thermal-hydraulic parameter	$\boldsymbol{GCI_{r_{32}}}$		
	Ø9.52 mm	**Ø12.70 mm**	**Ø19.05 mm**
Nusselt number, Nu	0.104 %	0.040 %	0.136 %
Pressure loss, ΔP	1.240 %	0.712 %	1.810 %
Mass flow, $\dot{m}$	0.213 %	0.017 %	1.320 %

Tetrahedral elements with local growth control methods were chosen to discretize the computational, as shown in Figure 3 (a). Prismatic elements were created on the tube wall to aid in the convergence process and improve capturing of the wall effects. Figure 3 (b) shows the prismatic elements of the intermediate mesh of the tube. The Orthogonal Quality Criteria and Skewness were satisfied to ensure the mesh quality.

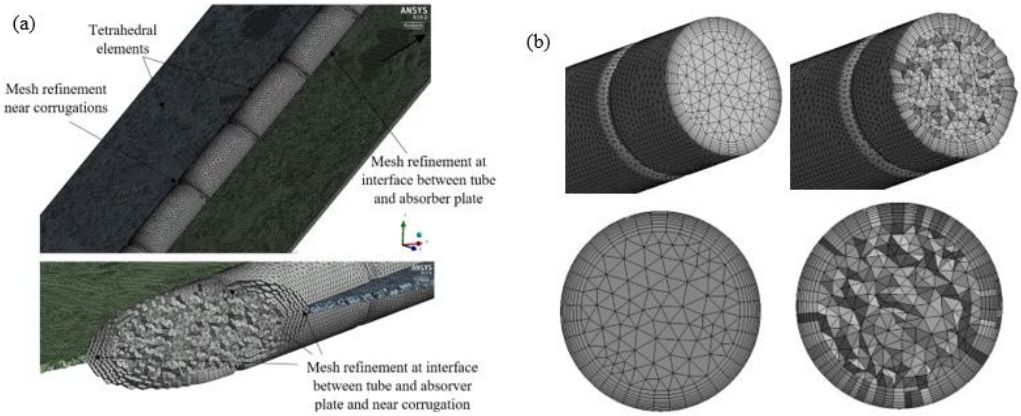

Figure 3. Mesh. (a) Refinement details. (b) elements 2D and 3D.

The validation of the numerical model is carried out by comparing numerical and theoretical values of the Nusselt number for configurations with tubes without corrugations and absorber plates, inclined at 30° and 45°. This is done due to the lack of correlations in the literature that show good predictability of important parameters associated with the numerical modeling of the inclined flat plate collector. The proposed equation by Sieder and Tate (1936), valid for laminar flow, with constant wall temperature and combined input, defined by Eq. (14), is used to correlate the results. The correlation precise the data with standard deviation of 19% for the heating of the water process.

$$Nu = 1.86(Gz)^{1/3}\left(\frac{\mu_m}{\mu_w}\right)^{0.14} \text{ para Gz} > 10 \tag{14}$$

The correlation calculates the Nusselt number as a function of the Graetz number (Gz), defined by Eq. (15).

$$Gz = RePr\left(\frac{D}{l}\right) \tag{15}$$

On the surface of the tubes, temperature of 310K was taken into consideration for validation. In this condition, the convection heat transfer coefficient is determined by the logarithmic average of the temperature differences, defined by Eq. (16). Table 3 shows the comparison of numerical and theoretical results.

$$\Delta T_{ml} \equiv \frac{\Delta T_{sai} - \Delta T_{ent}}{\ln(\Delta T_{sai}/\Delta T_{ent})} \tag{16}$$

Table 3. Comparation between numerical and theoretical results.

Tilt angle		**Nusselt number, Nu**		
		Ø9.52 mm	**Ø12.70 mm**	**Ø19.05 mm**
30°	Correlation	7.664	9.981	13.520
	Numerical	7.729	10.670	15.009
	Deviation	0.8%	6.5%	9.9%
45º	Correlation	8.181	10.578	14.164
	Numerical	7.755	10.328	14.113
	Deviation	-5.5%	-2.4%	-0.4%

3. RESULTS AND DISCUSION

3.1 Impact of diameter and tilted angle on non-corrugated configurations

The heat transfer rate between tube configurations with and without absorber plates inclined at 45º is shown in Figure 4 (a). For configurations with absorber plates, tubes with larger diameters provide a modest increase in the rate of heat transfer. The result presented by tube with a diameter of 19.05 mm is 3.5% and 5.1% higher than the configurations with a diameter of 12.70 mm and 9.52 mm, respectively.

The difference in heat transfer rate between configurations with and without absorber plates is more significant. The heat absorption capacity of the collector with absorber plates and 9.52 mm diameter tube is 3.5 times greater than the absorption capacity of the collector without the plates. The impact of inclination angle on configurations with absorber plates is negligible, as shown in Figure 4 (b).

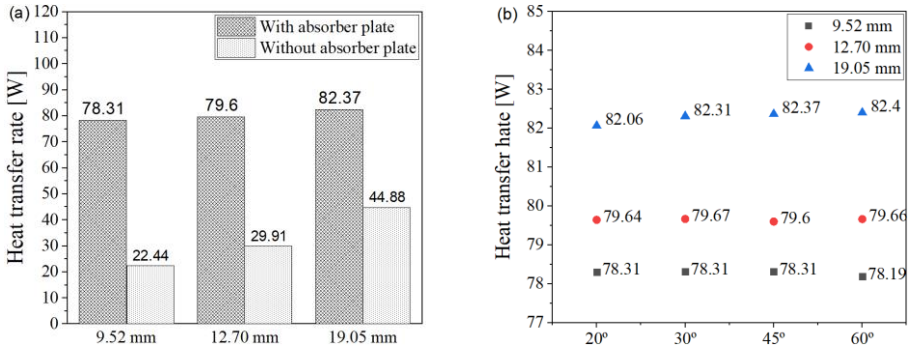

Figure 4. Impact of tube diameter and tilt angle on heat transfer rate. (a) Comparison between configurations with and without absorber plate for 45º inclination. (b) Impact of tilt angle for configurations with absorber plates.

Figure 5 (a-b) shows that tubes with larger diameters promote an increase of the mass flow and a reduction in pressure drop. Considering variation of the angle of inclination between tubes of the same diameter, the greatest percentage difference, both for mass flow and for the pressure drop, is obtained when comparing the results of the inclined configurations at 20° and 60°, equivalent to 50%. However, the impacts on both parameters are more pronounced as the tube diameter is increased. The 9.52 mm tubes, which give the lowest flow rate among the analyzed configurations, have a mass flow rate three times lower than the 19.05 mm diameter tubes for the same tilted angle. For the pressure drop, the result of tubes with a diameter of 19.52 mm is 5 times lower than that of tubes with a diameter of 9.52 mm.

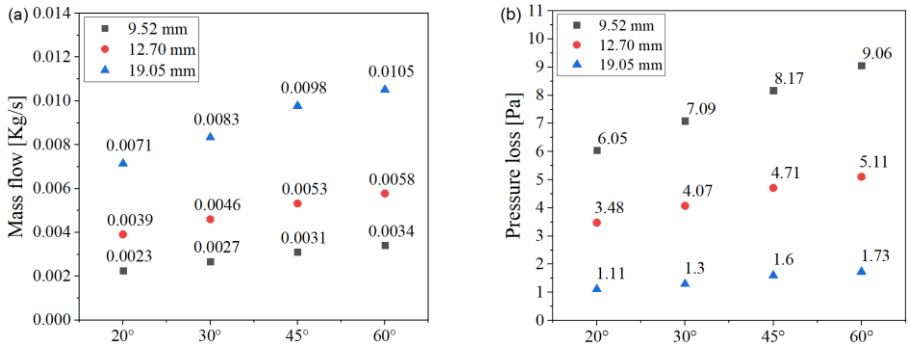

Figure 5. Impact of tube diameter and tilt angle. (a) Mass flow (b) Pressure loss.

In passive systems, the thermo-hydraulic performance of collectors is intrinsically related to the tube diameter. The mass flow is decreased since there is no external pumping source to juxtapose the impact of shear stresses produced by tubes with lower diameters. The Reynolds number and the friction factor are affected for the same reason, but in an inversely correlated way, as shown in Figure 6 (a-b). The tube with a diameter of 19.05 mm and an angle of 60° provides the system with the greatest Reynolds number (784) and the lowest friction factor (0,048) among the evaluated configurations. The reduction in the friction factor in response to the increase in the inclination angle can be attributed to the decrease in the perpendicularity between the main (axial) flow and the vertical flow of natural convective currents.

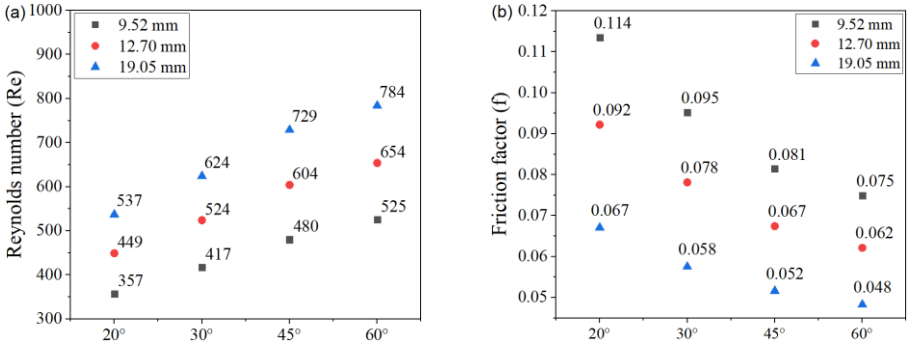

Figure 6. Impact of tube diameter and tilt angle. (a) Reynolds number. (b) Friction factor.

In quantitative terms, tubes with larger diameters increase the Nusselt number for the same tilted angle. However, increasing the angle of inclination for tubes with the same diameter reduces the parameter, as shown in Figure 7. For configurations inclined at 20º, the average Nusselt number for a tube with a 19.05 mm diameter is 37.5% higher than the result presented by the 9.52 mm. For angles of 30°, 45° and 60° the difference corresponds to 39%, 41% and 45%, respectively.

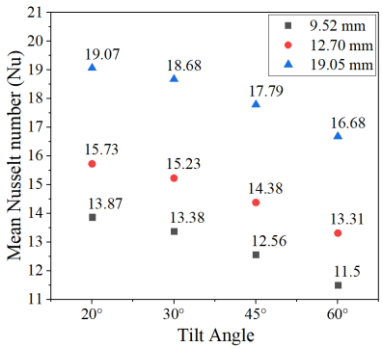

Figure 7. Impact of tube diameter and tilt angle on mean Nusselt number.

The thermo-hydraulic performance of the configurations is defined by the ratio between the Nusselt number and the friction factor. Figure 8 shows the increase in thermo-hydraulic performance associated with the increase in tube diameter and inclination angle. On average, the 19.05 mm diameter tubes offer thermo-hydraulic performance for the evaluated angles that is 2.3 times larger than the 9.52 mm tubes. For tubes of the same diameter, increasing the angle of inclination from 20° to 30° provides 14.5% of increase, while 30° to 45° the gains is equivalent at 9.5%. The behavior of the thermo-hydraulic performance stabilizes at an angle of 45º. From then, stabilization in the behavior of the thermo-hydraulic performance is observed.

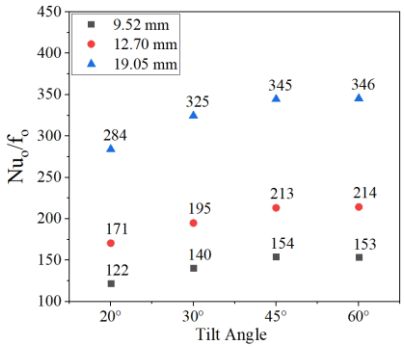

Figure 8. Thermo-hydraulic performance of non-corrugated configurations.

3.2 Impact of corrugated tubes in a thermosyphon system

Although the results obtained from the configurations inclined at 45° and 60° are comparable, the configuration with a diameter tube of 19.05 mm inclined at 45° is utilized for the evaluation of the enhancement of heat transfer promoted

by the corrugations because it has a higher thermal-hydraulic performance and heat transfer rate than others. Table 4 summarizes the physical characteristics of the evaluated corrugations.

Table 4. Corrugations characteristics.

Configuration	Corrugation heigh (*e*) [mm]	Corrugation pitch (*p*) [mm]
R5 P10	0.476	10
R5 P20	0.476	20
R10 P10	0.952	10
R10 P20	0.952	20

Figure 9 (a) shows the impact of corrugated configurations on heat transfer rate. Although the corrugated configurations did not provide significant improvements to the heat transfer rate, they did not negatively affect the parameter. On the other hand, the use of corrugations promoted enhancements in the convective heat transport process. Figure 9 (b) shows a comparison of the Nusselt number results for corrugated and non-corrugated configuration (reference). The results demonstrate that the convective heat transfer process among configurations with the same corrugation height benefits from raising the corrugation pitch. However, for configurations with a pitch of 10 mm, increasing the corrugation height is harmful to the heat transfer process for all examined profiles.

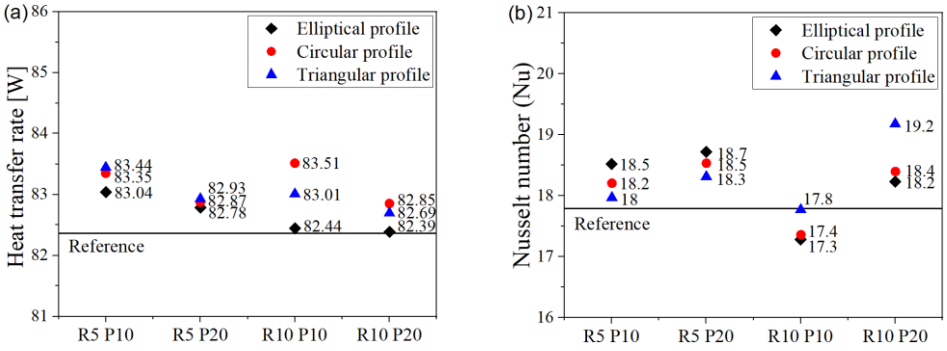

Figure 9. Impact of corrugated configurations. (a) Heat transfer rate; (b) Nusselt number.

The elliptical and circular profile configurations with a pitch of 20 mm showed a reduction in the convective heat transfer capacity with the increase in the corrugation height. However, for the triangular profile, the increase in the corrugation height favored the convective heat transfer process. The configuration R10 P20 with triangular profile increased the Nusselt number by 8% in relation to the non-corrugated configuration subjected to the same conditions.

The impact of corrugations on the thermo-hydraulic performance is evaluated by the ratio between the Nusselt number and the friction factor obtained by the corrugated configurations (Nu and f) and non-corrugated configuration (Nu_o and f_o). Figure 10 shows that tubes with a triangular corrugation profile provide superior thermo-hydraulic performance than the other evaluated configurations. The configuration with triangular profile R5 P10, especially, increased the thermo-hydraulic performance of the system by 25%. However, the bad sizing of the height or pitch of the corrugations can lead to a reduction in the convective heat transfer capacity and in the thermo-hydraulic performance of systems when they operate exclusively under the thermosyphon effect. The results presented by the R10 P10 configurations illustrate this observation.

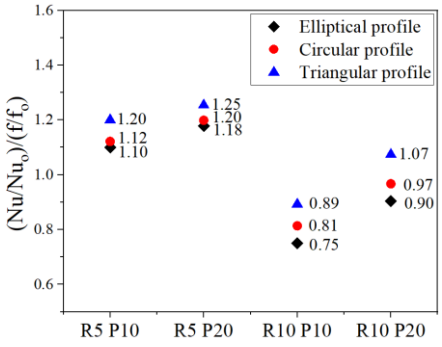

Figure 10. Thermal-hydraulic performance of corrugated configurations.

The increase in thermo-hydraulic performance is associated with a lower pressure drop, and consequently, a lower friction factor provided by the triangular profile in the evaluated configurations, as shown by the data in Table 5.

Table 5. Results of corrugated configurations.

Configuration	Profile	Mass Flow [kg/s]	Pressure loss [Pa]	Reynolds number	Friction factor
R5 P10	Elliptical	0.008018	1.0198	601	0.0489
	Circular	0.008084	0.9994	606	0.0471
	Triangular	0.007990	0.9004	599	0.0434
R5 P20	Elliptical	0.008180	1.0017	613	0.0461
	Circular	0.008200	0.9794	614	0.0449
	Triangular	0.008137	0.9094	609	0.0423
R10 P10	Elliptical	0.007170	1.1154	538	0.0668
	Circular	0.007306	1.0727	549	0.0619
	Triangular	0.007330	1.0079	550	0.0578
R10 P20	Elliptical	0.007489	1.0655	562	0.0585
	Circular	0.007644	1.0473	573	0.0552
	Triangular	0.007639	0.9820	573	0.0518

Despite the use of corrugations did not result in appreciable increases in the rate of heat transfer, the method showed promise for enhancing convective heat transfer capacity and improving thermo-hydraulic performance in systems with concentric absorber plates that operate exclusively under the thermosyphon effect.

4. CONCLUSION

In this work, the heat transfer process in a flat plate solar collector with corrugated tubes is evaluated. The heat transfer rate, thermo-hydraulic performance and convective heat transfer capacity are the main parameters analyzed. Numerical analysis first evaluates the impact of tube diameter (Ø9.52 mm, Ø12.70 mm and Ø19.05 mm) and inclination angle (20°, 30°, 45° and 60°) on a traditional thermosyphon system, with non-corrugated tubes. Subsequently, the impact provided by transversal corrugations with a triangular, circular and elliptical profile, with different configurations of height and pitch, is compared with the result obtained by the configuration of a tube with a diameter and angle of inclination that promoted a greater thermo-hydraulic performance and rate of heat transfer than others.

The most important results are summarized as follows:

1. Solar collectors with concentric absorber plates show higher heat transfer rates by up to 3.5 times the results obtained by configurations that do not have absorber plates.
2. For non-corrugated configurations with the same angle of inclination, increasing the tube diameter from 9.52 mm to 19.05 mm improves the heat transfer rate of the system by 5.1%. On the other hand, for the same tube diameter, increasing the angle of inclination does not promote significant gains.
3. The system's thermo-hydraulic performance up to angle of 45° is significantly improved by the increase in the angle of inclination and tube diameter. From than, stabilization in the behavior of the thermo-hydraulic performance is observed.
4. The configurations corrugated that was tested not offered appreciable increases in heat transfer rate. However, the triangular profile R10 P20 boosted the thermosyphon system's convective heat transfer capacity by 8%, while the R5 P20 configuration improved the system's thermo-hydraulic performance by 25%.
5. For configurations with the same pitch, an increase in the height of the corrugation has a detrimental effect on the mass flow, pressure drop, and friction factor. As a result, the thermo-hydraulic performance of the system is impaired, which may generate results below unity. However, increasing the pitch and maintaining the same corrugation height can improve the convective heat transfer capability of the system, in addition to improving thermo-hydraulic performance.

5. REFERENCES

ABRASOL, 2022, Boletim 33 – Nov/2022, Brazilian Association of Thermal Solar Energy ABRASOL, São Paulo, https://abrasol.org.br/boletim-i-novembro-i-no33-2022/. Accessed 18 December 2022.

Agunlejika, E. O., Langston, P., Azzopardi, B. J., Hewakandamby, B. N., 2016, Flow instabilities in a horizontal thermosyphon reboiler loop, Experimental Thermal and Fluid Science, Vol. 78, p. 90-99.

Andrade, F., Moita, A. S., Nikulin, A., Moreira, 2019, Experimental investigation on heat transfer and pressure drop of internal flow in corrugated tubes, International Journal of Heat and Mass Transfer, Vol. 140, p. 940–955.

Barba, A., Rainieri, S., Spiga, M., 2002, Heat transfer enhancement in a corrugated tube, International Communications in Heat and Mass Transfer, Vol. 29, n. 3, p. 313–322.

Barth, T. J., Jespersen, D. C., 1989, The design and application of upwind schemes on unstructured meshes, AIAA Paper No. 89-0366, 27th AIAA Aeroespace Sciences Metting, Reno, NV.

Celik, I. B., Ghia, U., Roache, P. J., Freitas, C. J., Coleman, H., Raad, P. E., 2008, Procedure for estimation and reporting of uncertainty due to discretization in CFD applications. Journal of Fluids Engineering, Transactions of the ASME, Vol. 130, n. 7, p. 0780011–0780014.

Chen, C., Wu, Y., Wang, S., Ma, C., 2013, Experimental investigation on enhanced heat transfer in transversally corrugated tube with molten salt, Experimental Thermal and Fluid Science, Vol. 47, p. 108–116.

Cruz, G. G., Mendes, M. A. A., Pereira, J. M. C., Santos, H., Nikulin, A., Moita, A. S., 2021, Transfer Experimental and numerical characterization of single-phase pressure drop and heat transfer enhancement in helical corrugated tubes, International Journal of Heat and Mass, Vol. 0., 121632.

Du, J., Hong, Y., Huang, S., Ye, W., Wang, S., 2018, Laminar thermal and fluid flow characteristics in tubes with sinusoidal ribs, International Journal of Heat and Mass Transfer, Vol. 120, p. 635–651.

García, A., Solano, J. P., Vicente, P. G., Viedma, A., 2012, The influence of artificial roughness shape on heat transfer enhancement: Corrugated tubes, dimpled tubes and wire coils, Applied Thermal Engineering, Vol. 35, n. 1, p. 196–201.

Ghasemi, E., Soleimani, S., Bararnia, H., 2012, Natural convection between a circular enclosure and an elliptic cylinder using Control Volume based Finite Element Method, International Communications in Heat and Mass Transfer, Vol. 39, n. 8, p. 1035–1044.

Jaisankar, S., Radhakrishnan, T. K.; Sheeba, K. N, 2011, Experimental studies on heat transfer and thermal performance characteristics of thermosyphon solar water heating system with helical and Left-Right twisted tapes, Energy Conversion and Management, Vol. 52, n. 5, p. 2048–2055.

Jamar, A., Majid, Z. A. A., Azmi, W. H., Norhafana, M., Razak, A. A., 2016, A review of water heating system for solar energy applications, International Communications in Heat and Mass Transfer, Vol. 76, p. 178–187.

Mohammed, H. A., Abbas, A. K., Sheriff, J. M., 2013, Influence of geometrical parameters and forced convective heat transfer in transversely corrugated circular tubes, International Communications in Heat and Mass Transfer, Vol. 44, p. 116–126.

Müller, S., Giovannetti, F., Reineke-Koch, R., Kastner, O., Hafner, B., 2019, Simulation study on the efficiency of thermochromic absorber coatings for solar thermal flat-plate collectors, Solar Energy, Vol. 188, n. March, p. 865–874.

Pereira, E. B., Martins, F. R., Gonçalves, A. R., Costa, R.S., Lima, F. J. L., Ruther, R., Abreu, S. L., Tiepolo, G. M., Pereira, S. V., Souza, J. G., 2017, Atlas Brasileiro de Energia Solar, INPE, 2.ed., ISBN 978-85-17-00089-8, Julho 2017, São José dos Campos, São Paulo, Brasil

Rainieri, S., Farina, A., Pagliarini, G., 1996, Experimental investigation of heat transfer and pressure drop augmentation for laminar flow in spirally enhanced tubes, Proceedings of the 2nd European Thermal-Sciences and 14th UIT National Heat Transfer Conference, Edizioni, p. 203–209.

Rainieri, S., Pagliarini, G., 2002, Convective heat transfer to temperature dependent property fluids in the entry region of corrugated tubes, International Journal of Heat and Mass Transfer, Vol. 45, n. 22, p. 4525–4536.

Sieder, E. N., Tate, G. E., 1936, Heat transfer and pressure drop of condensation of hydrocarbons in tubes, Heat and Mass Transfer/Waerme- und Stoffuebertragung, Vol. 55, n. 1, p. 33–40.

Shukla, R., Sumanthy, K., Erickson, P., 2013. Recent advances in the solar water heating systems: A review, Renewable and Sustainable Energy Reviews, Vol. 19, p. 173–190.

Solar Heat World Wide, 2022, *Global Market Development and Trends 2021*, AEE – Institute for Sustainable Technologies 8200 Gleisdorf, Austria, https://www.iea-shc.org/Data/Sites/1/publications/Solar-Heat-Worldwide-2022.pdf. Accessed 10 August 2022

Vicente, P. G., García, A., Viedma, A., 2004, Mixed convection heat transfer and isothermal pressure drop in corrugated tubes for laminar and transition flow, International Communications in Heat and Mass Transfer, Vol. 31, n. 5, p. 651–662.

Vicente, P. G., García, A., Viedma, A., 2004, Experimental investigation on heat transfer and frictional characteristics of spirally corrugated tubes in turbulent flow at different Prandtl numbers, International Journal of Heat and Mass Transfer, Vol. 47, n. 4, p. 671–681.

Vijay, R., Vijayakumar, P., Kumaresan, G., Kumar, S. G., 2021, Performance study of flat plate solar collector integrated with twisted tape inserts, Materials Today: Proceedings, Vol. 45, p. 1222–1226.

Visa, I., Moldovan, M., Duta, A., 2019, Novel triangle flat plate solar thermal collector for facades integration, Renewable Energy, Vol. 143, p. 252–262.

Zayed, M. E., Zhao, J., Elsheikh, A. H., Du, Y., Hammad, F. A., Ma, L., Kabeel, A. E., Sadek, S., 2019, Performance augmentation of flat plate solar water collector using phase change materials and nanocomposite phase change materials: A review, Process Safety and Environmental Protection, Vol. 128, p. 135–157.

6. RESPONSIBILITY NOTICE

The authors are the only responsible for the printed material included in this paper.